Investigation of the gas phase reactivity of the 1-adamantyl radical using a distonic radical anion approach

David G. Harman and Stephen J. Blanksby*

Received 20th July 2007, Accepted 10th September 2007
First published as an Advance Article on the web 19th September 2007
DOI: 10.1039/b711156h

The gas phase reactions of the bridgehead 3-carboxylato-1-adamantyl radical anion were observed with a series of neutral reagents using a modified electrospray ionisation linear ion trap mass spectrometer. This distonic radical anion was observed to undergo processes suggestive of radical reactivity including radical–radical combination reactions, substitution reactions and addition to carbon–carbon double bonds. The rate constants for reactions of the 3-carboxylato-1-adamantyl radical anion with the following reagents were measured (in units 10^{-12} cm^3 molecule^{-1} s^{-1}): $^{18}O_2$ (85 ± 4), NO (38.4 ± 0.4), I_2 (50 ± 50), Br_2 (8 ± 2), CH_3SSCH_3 (12 ± 2), styrene (1.20 ± 0.03), $CHCl_3$ (H abstraction 0.41 ± 0.06, Cl abstraction 0.65 ± 0.1), $CDCl_3$ (D abstraction 0.035 ± 0.01, Cl abstraction 0.723 ± 0.005), allyl bromide (Br abstraction 0.53 ± 0.04, allylation 0.25 ± 0.01). Collision rates were calculated and reaction efficiencies are also reported. This study represents the first quantitative measurement of the gas phase reactivity of a bridgehead radical and suggests that distonic radical anions are good models for the study of their elusive uncharged analogues.

Introduction

Bridgehead radicals are fascinating molecules with their rigid structures making them exceptional probes of fundamental chemistry. Invariant intermolecular distances and bond angles allow these species to be utilised in the exploration of subjects such as orbital and bond interactions, as well as conformational and substituent effects upon reactivity.[1] Bond angles for a series of bridgehead radicals have been obtained by electron spin resonance (ESR) spectroscopy from measurement of ^{13}C hyperfine tensors and at 77 K the 1-adamantyl radical is estimated to have a bridgehead C–C–C angle of 113.6°.[2] This experimentally derived value is congruent with gas phase structure calculations that predict a bond angle of 113° for the 1-admantyl radical using density functional methods.[3,4] Such deviation from the 118° for the near planar *tert*-butyl radical,[5–7] demonstrates the degree of pyramidalisation around the bridgehead radical. Further computational studies predict that as the geometry of a carbon-centred radical deviates increasingly from its most stable planar conformation, the energy increases since spin delocalisation mechanisms such as resonance and hyperconjugation are compromised.[8] These calculations also predict an increase in the bridgehead C–H bond dissociation energy in strained hydrocarbons as a function of increases in the sum of the H–C–C bond angles.[8] Such calculations are supported by experimental measurements of spin density at radical centres that reveal an increase from 83 to 88% upon transition from 1-adamantyl to, the even further distorted, 1-bicyclo[1.1.1]pentyl radical.[2] In a previous computational study from our own laboratory[4] we have shown that the 1-adamantyl radical **2** is pyramidal about C_1 but has shorter Cα–Cβ bonds, longer Cβ–Cγ bonds, larger Cβ–Cα–Cβ angles and smaller Cα–Cβ–Cγ angles than adamantane **1** (Scheme 1). These observations

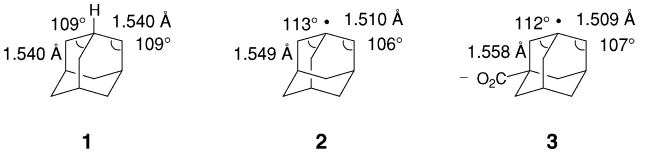

1 **2** **3**

Scheme 1

are supported by previous calculations by Schaefer and co-workers[3] and are consistent with the radical centre being slightly flattened by H–Cβ–Cα hyperconjugation.

In solution, bridgehead radicals undergo the expected suite of free radical reactions including: (i) addition to multiple bonds, (ii) abstraction of hydrogen or halogen atoms, (iii) coupling with other radicals, and (iv) β-scission promoted rearrangements, although such isomerisations are facile only for species containing 3- or 4-membered rings.[2] Pyramidalisation of a carbon-centred radical at a bridgehead carbon might be expected to increase its rate of reaction relative to unconstrained tertiary radicals. Alternatively, the strained geometry about the bridgehead radical centre might retard reactions in some instances due to frontier orbital effects.[9] To this point, however, a paucity of empirical data has provided a significant impediment to the rigorous exploration of such ideas. In one of the few experimental comparisons available, rate constants for the addition of bicyclo[1.1.1]pent-1-yl radical to α-methylstyrene (1.4×10^7 M^{-1} s^{-1} or 2.32×10^{-14} molecule^{-1} cm^3 s^{-1}) and hydrogen atom abstraction from 1,4-cyclohexadiene (4.6×10^5 M^{-1} s^{-1} or 7.64×10^{-16} molecule^{-1} cm^3 s^{-1}) were measured at 25° C by laser flash photolysis.[10] These rate constants are, respectively, 200 and 50 times greater than those for the same reactions of *tert*-butyl, confirming that for these reactions the bridgehead radical is more reactive than its unconstrained analogue.

Bridgehead radicals provide a unique model in which to investigate the intrinsic reactive properties of carbon-centred radicals. Gas phase radical reactions, however, have typically been

Department of Chemistry, University of Wollongong, Gwynneville, NSW 2522, Australia. E-mail: blanksby@uow.edu.au

difficult to study for several reasons: the occurrence of secondary chemistry, high reaction rates, instability of intermediates and difficulties with detection. Yet, important radical-mediated processes such as combustion of hydrocarbons and the production of photochemical smog often lack solid evidence in support of postulated reaction schemes and putative reaction intermediates.[11] In this paper, we describe how it is now possible to study a single step in the reactions of a bridgehead radical using a combination of distonic radical anions and linear ion trap mass spectrometry.

Ion trap mass spectrometry allows gas phase ions to be isolated (purified) by mass selection, contained (stored) within electric fields for periods of time and fragmented (energised) by collision with an inert bath gas to yield smaller ions which provide structural information. Product ions may then be trapped and fragmented further, often several times. A significant recent development has been the conversion of ion trap mass spectrometers into 'gas phase synthetic reactors' by the introduction of reagents into the trap atmosphere such that ion–molecule reactions may be observed.[12,13] For our purposes, the technique has the following strengths: the reactions of one type of ion at time may be studied, like-charge repulsion prevents ions from reacting with each other (no interference with radical termination events), and reaction rate data may be obtained.

As mass spectrometers detect only ionic species, it was necessary to introduce a charged functional group into the 1-adamantyl radical. However, the charge and radical centres must remain separate—both spatially and electronically—in order not to interfere with the reactivity of the radical. The charge must be relatively inert, to avoid a predominance of ionic chemistry. Accordingly, the *distonic*[14] radical anion 3-carboxylato-1-adamantyl **3** (Scheme 1) was a logical target of choice. The distonic approach to radical reactivity has been employed previously by the groups of Kenttämaa,[15–17] Kass[18] and O'Hair.[19–21]

The calculated structures of the 1-adamantyl radical **2** and 3-carboxylato-1-adamantyl radical anion **3** reveal that comparable bond lengths and angles are very similar, suggesting that distonic ion **3** makes an excellent model to study the reactivity of **2** (Scheme 1).[4] Radical anion **3** can be generated by oxidative decarboxylation of the 1,3-adamantane dicarboxylate dianion **4** (Scheme 2),[4] in a similar manner to the production of distonic 4-carboxylato-1-phenyl radical anions from benzene dicarboxylate dianions.[18] However, low yields from this process have been encountered in the presence of some gas-phase reagents due to the preponderance of ionic reactions of the dianion. A convenient solution to this problem lay in the derivatisation of one carboxylic acid group of 1,3-adamantane dicarboxylic acid to its *N*-acyloxypyridine-2-thione—or colloquially, Barton ester—functional group.[22] Della and Tsanaktsidis have successfully adopted this function in the generation of radical intermediates for the synthesis of bridgehead halides.[23] In solution, treatment of an *N*-acyloxypyridine-2-thione with a radical initiator, or subjection to thermolysis or photolysis, is known to generate a carbon centred radical by homolysis of the N–O bond, then subsequent rapid decarboxylation.[22] Our computational estimate of the bond dissociation energy of the weak N–O bond of methyl Barton ester is 65 kJ mol^{-1}. Preparation of the adamantyl Barton ester acid was accomplished in one step from 1,3-adamantane dicarboxylic acid by adaptation of a standard method.[24] Electrospray ionisation of a methanolic solution of the Barton ester in the mass spectrometer

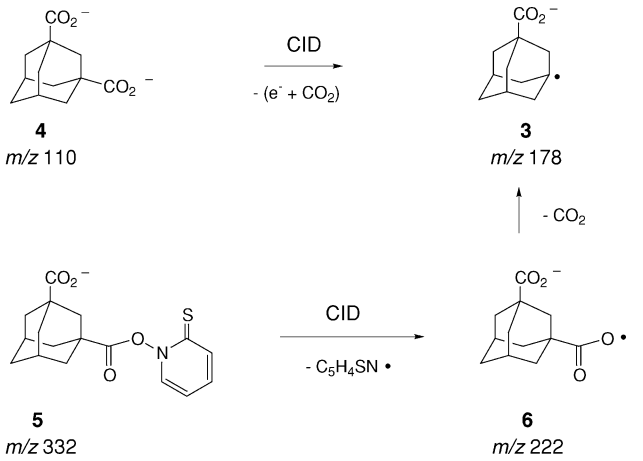

Scheme 2

resulted in the observation of carboxylate anion **5** at *m/z* 332 (Scheme 2). This ion was trapped then subject to collision induced dissociation (CID), which produced the desired radical ion **3** of *m/z* 178 efficiently, demonstrating that Barton esters are also effective in the generation of gas phase radicals. The intermediate acyloxy radical **6** was not observed due to the extremely rapid rate of decarboxylation.[4] In the present study, reactions of **3** with nine reagents were observed and occurred overall in a manner similar to what would be predicted from a knowledge of solution phase chemistry. Second order rate constants were measured and reaction efficiencies were estimated based on theoretical collision rates.

Results and discussion

Validation of kinetic measurements

As a test of the accuracy of our experimental approach, we measured the rate constants of three ion–molecule reactions whose kinetics had previous been determined by flowing afterglow-selected ion flow tube (FA-SIFT) mass spectrometry (Table 1).[25,26] These reactions were: (1) the displacement of iodide from iodomethane by $^{35}Cl^-$ (eqn (1)), (2) the displacement of iodide from iodomethane by $^{79}Br^-$ (eqn (2)), and (3) the bimolecular reaction of 1,1,1,3,3,3-hexafluoroisopropoxide ion with bromoethane (eqn (3)). Although this last reaction yields products resulting from both a substitution and elimination reaction (eqn (3a) and (3b), respectively), Br^- (*m/z* 79/81) is the only charged product detected in this experiment and thus the rate constant determined is in fact the sum of the rate constants of two second-order processes. As a check of accuracy with reactions of *radicals*, the rate

Table 1 Comparison of second order rate constants (k_2) for the ion–molecule reactions depicted in eqn (1)–(4), determined by the current ion trap method and by FA-SIFT or FT-ICR techniques

Reaction equation	k_2 by current ion trap method/cm^3 molecule^{-1} s^{-1}	Literature k_2/cm^3 molecule^{-1} s^{-1}	Literature method
(1)	$1.2 \pm 0.3 \times 10^{-10}$	$1.66 \pm 0.03 \times 10^{-10}$	FA-SIFT[25]
(2)	$3.0 \pm 0.4 \times 10^{-11}$	$2.89 \pm 0.09 \times 10^{-11}$	FA-SIFT[25]
(3)	$5.6 \pm 0.6 \times 10^{-12}$	$7.83 \pm 0.33 \times 10^{-12}$	FA-SIFT[25]
(4)	$3.75 \pm 0.1 \times 10^{-12}$	$8 \pm 4 \times 10^{-12}$	FT-ICR[15]

constant for the reaction of the distonic 3-carboxylato-1-phenyl radical anion (**7**) with dimethyl disulfide (eqn (4)) was determined and is compared to the value previously reported from Fourier transform ion cyclotron resonance (FT-ICR) mass spectrometry.[15] The results of kinetic measurements for the reactions shown in eqn (1)–(4) are presented in Table 1 and represent an average of at least three separate determinations, each under differing neutral concentrations. The uncertainties represent one standard deviation of the precision.

$$^{35}Cl^- + CH_3–I \rightarrow {}^{35}Cl–CH_3 + I^- \quad (1)$$

$$^{79}Br^- + CH_3–I \rightarrow {}^{79}Br–CH_3 + I^- \quad (2)$$

$$(CF_3)_2CH–O^- + CH_3CH_2–Br \rightarrow (CF_3)_2CH–O–CH_2CH_3 + Br^- \quad (3a)$$

$$(CF_3)_2CH–O^- + CH_3CH_2–Br \rightarrow (CF_3)_2CH–OH + CH_2{=}CH_2 + Br^- \quad (3b)$$

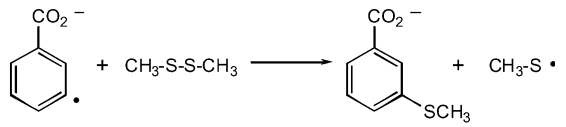

(4)

7

The measured rate constants obtained for reactions (1)–(3) agree favourably with the respective FA-SIFT values, considering that the absolute accuracy of the latter method is estimated at ±20%[26] and an estimation of accuracy of ion-trap derived rate constants of ±25%.[13] The measured rate constant for the reaction of a distonic radical anions (eqn (4)) of $3.75 \pm 0.1 \times 10^{-12}$ also agrees well with a value previously obtained by FT-ICR mass spectrometry of $8 \pm 4 \times 10^{-12}$ cm^3 molecule^{-1} s^{-1}.[15] The data suggest that the linear ion trap mass spectrometer used in this study is expected to provide highly reproducible gas phase rate measurements (high precision) and yield rate constants of reasonable absolute accuracy for the reactions of both closed-shell and radical ions with neutral reagents.

Verification of the structure of the radical

Before discussion of the reactions of the 3-carboxylato-1-adamantyl radical anion (**3**), it is important to establish that the putative structure shown in Scheme 1 is the correct connectivity of the ion observed at *m/z* 178 resulting from CID of the Barton ester anion **5**. We have previously addressed the possibility that the radical in question may instead be the ring-opened isomer **8** (Scheme 3).[4] Tertiary radical **8** is stabilised by resonance interactions with the adjacent carboxylate group and by relief of ring strain relative to **3**, thus making it the most likely structural alternative to **3**. Electronic structure calculations at the B3LYP/6-31+G(d)//HF/6-31+G(d) level of theory suggest that an activation energy of 81 kJ mol^{-1} must be overcome for conversion of **3** into **8**.[4] It was previously argued that this barrier was sufficiently large to prevent isomerisation given: (i) the gentle method of radical formation, (ii) the fact that CID does not produce energetic secondary collisions in ion traps and (iii) the rapid cooling (5–10 ms)[27,28] of ions by collisions with the helium

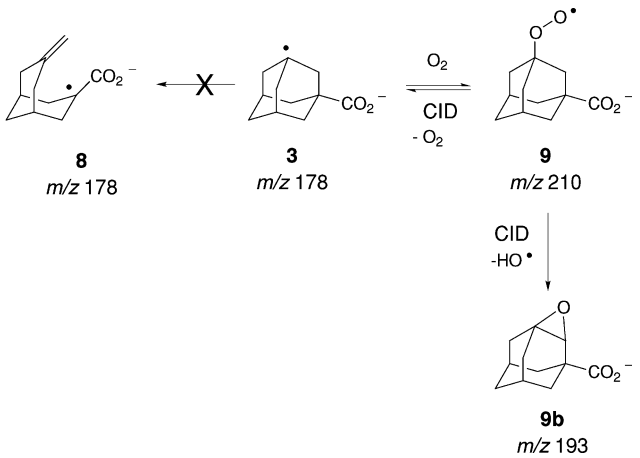

Scheme 3

buffer gas. Further experimental evidence for the bridgehead structure of **3** is presented below.

The ion at *m/z* 178 reacts with adventitious dioxygen inside the ion trap, forming an ion of *m/z* 210 that has been assigned as the peroxyl radical **9**.[4] When the latter ion is isolated and provided with additional energy in a CID experiment, the original progenitor ion at *m/z* 178 is reformed. Furthermore, when this new ion of *m/z* 178 is subsequently trapped (in an MS^5 experiment), it reforms *m/z* 210 at the same rate as initial peroxyl radical formation. Such observations are consistent with previous reports of the loss of dioxygen from the benzyl peroxyl radical forming the benzyl radical[29] and suggest that in this instance the structure of the adamantyl radical is unchanged following addition and subsequent removal of O_2. In addition, CID of the ion we have assigned to be **9** forms a small amount of *m/z* 193, corresponding to the 1,2-epoxyadamantane-3-carboxylate anion **9b** which forms by loss of hydroxyl radical (Scheme 3). If *m/z* 210 were the peroxyl radical of **8**, under CID one should expect also to see formation of *m/z* 177 *via* loss of hydroperoxyl radical, but none is observed.

To ensure that the structure of the radicals of *m/z* 178 formed by oxidative decarboxylation of the 1,3-adamantane dicarboxylate dianion **4** and by homolysis of the Barton ester carboxylate anion **5** were identical, the kinetics of their reaction with background oxygen were measured under identical conditions. The ratio of rate constants was $k_{Barton}/k_{dianion} = 0.98 \pm 0.05$, indicating that radical structures were identical. In addition, the kinetic plots were highly linear ($R^2 = 0.9983$ and 0.9994 respectively) and reaction to immeasurably small ion counts of *m/z* 178 was evident at large reaction times, indicating that this ion population consists of the single isomer **3** not a mixture of **3** and **8**.

The distonic radical ion of *m/z* 178 reacts with molecular iodine to yield an ion of *m/z* 305, attributed to 3-iodoadamantane-1-carboxylate anion **10** (Scheme 4). Commercial adamantanecarboxylic acid was converted to 3-hydroxyadamantanecarboxylic acid **11** by treatment with alkaline, aqueous potassium permanganate.[30] Subsequent treatment of **11** with aqueous HI yielded 3-iodoadamantanecarboxylic acid **12** quantitatively (Scheme 4).

Fig. 1 depicts comparative spectra resulting from CID of *m/z* 305 for the product resulting from reaction between radical **3** and iodine (Fig. 1a) and for authentic 3-iodoadamantanecarboxylate

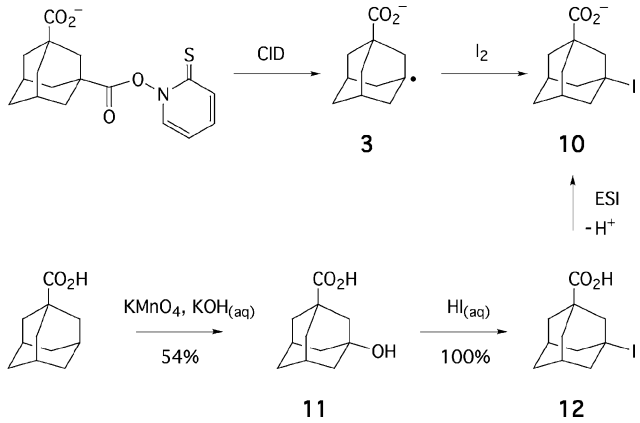

Scheme 4

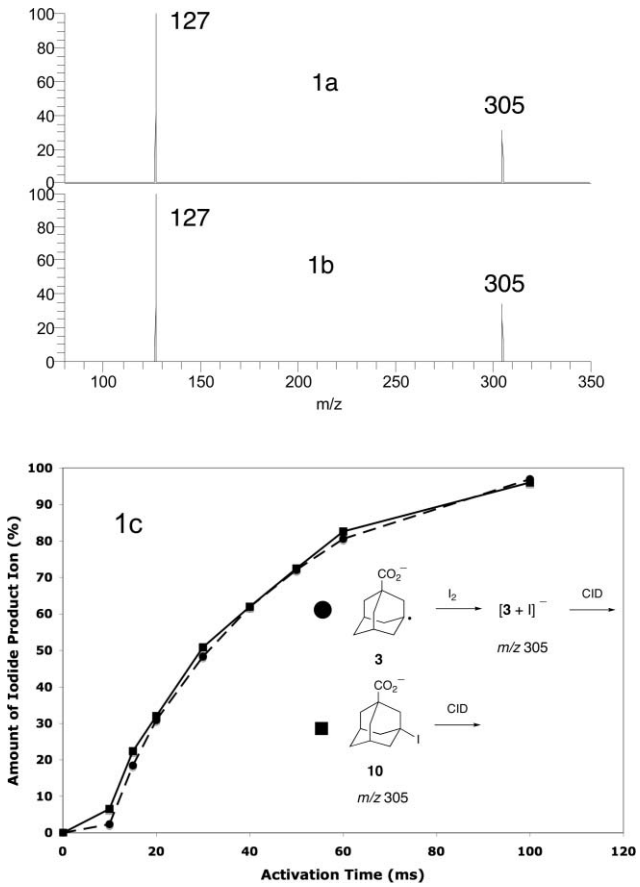

Fig. 1 Comparative mass spectra for CID of m/z 305 at a normalised collision energy of 15 arbitrary units and reaction time 50 ms. Spectrum (a) is of the authentic 3-iodoadamantanecarboxylate anion **10** and (b) the trapped product resulting from the reaction between radical **3** and iodine. (c) Comparison of the amount of iodide product ion formed *versus* activation time for CID at normalised collision energy 15. The solid curve represents data for authentic 3-iodoadamantanecarboxylate **10** and the dashed curve those for the product ion resulting from reaction of 1-adamantyl-3-carboxylate radical ion **3** with iodine inside the ion trap.

10 (Fig. 1b), generated by deprotonation of parent acid **12**. Both spectra were obtained with nominally identical iodine vapour concentrations since the presence of massive neutrals in the trap imparts greater collision energy to an ion given the same applied excitation amplitude. It is clear that the spectra look similar since the only product detected is iodide ion at m/z 127. In fact, the iodide ion remained the only product over the range of collision energies. Fig. 1c illustrates the comparison between the CID spectra for the authentic and gas-phase synthesized species at collision energy 15 (arbitrary units) at activation times ranging from 0–100 ms, representing a wide internal energy distribution. Data are expressed as iodide ion abundance as a proportion of the total ion count (*i.e.*, normalized ion counts) *versus* activation time. Data points for the trap-synthesized product ion and the authentic iodocarboxylate anion **10** compare favourably at all activation times, indicating that the ions of m/z 305 have identical structure. This evidence strongly supports the structure assigned to **3**, confirming that the adamantane ring system has not opened upon formation of the radical nor during subsequent reactions. Analogous experiments were also undertaken using the reagent bromine instead of iodine. Authentic 3-bromoadamantanecarboxylic acid was obtained by HBr treatment of **11**. Comparison of CID spectra at several collision energies indicated that the product ion resulting from reaction of radical **3** with bromine was entirely consistent with authentic 3-bromo-1-adamantanecarboxylate (data not shown). Thus, data from several experiments are consistent with the structure of the ion at m/z 178 being that of a bridgehead radical **3** and not the ring opened isomer **8**.

Reactions of the bridgehead radical

Reactions of the distonic bridgehead radical ion **3** with nine reagents were observed and their rate constants determined at 307 ± 1 K, the ambient temperature of the ion trap section of the mass spectrometer. It has been demonstrated that for low Q values (such as 0.25, used for these experiments) the effective temperature of ions held at zero collision energy inside an ion trap is approximately equivalent to the temperature of the buffer gas, and hence the temperature of the gas inlet to the trap itself.[31,32] Gronert has determined the effective temperature of ions contained within a three dimensional ion trap (from the same manufacturer as the linear trap employed herein) to be 310 ± 20 K, by measurement of the equilibrium constant of a complexation reaction displaying very large temperature dependence.[32] Collision rates z have been calculated at 307 K by average dipole orientation (ADO) theory[33] using an available Fortran routine[34] to enable reaction efficiencies to be estimated. Collision rates for ion–molecule reactions exceed those for comparable uncharged systems and are variable because they depend upon the mass of the reagent and attractive intermolecular forces between the neutral reagent and the ion. Reaction efficiencies Φ are calculated by dividing the empirical rate constants k_2 by theoretical collision rates z and are expressed as a percentage. Reaction rate constants and calculated reaction efficiencies are presented in Table 2.

Radical–radical combination reactions

Gross and co-workers have previously observed the gas phase addition of 32 Da to an ethylpyridinium radical cation in the presence of oxygen.[35] This observation was attributed to the radical–radical combination of the β-distonic radical cation and dioxygen to form

Table 2 Kinetic data, including second order rate constants (k_2), for the reaction at 307 ± 1 K of 3-carboxylato-1-adamantyl radical (**3**) with neutral reagents. Uncertainties represent one standard deviation

Reagent	Reaction	Rate constant k_2/cm^3 molecule^{-1} s^{-1}	Collision rate z/cm^3 molecule^{-1} s^{-1}	Efficiency Φ (%)
$^{18}O_2$	radical combination	$8.5 \pm 0.4 \times 10^{-11}$	5.4×10^{-10}	16
NO	radical combination	$3.84 \pm 0.04 \times 10^{-11}$	6.1×10^{-10}	5.7
I_2	I abstraction	$5 \pm 5 \times 10^{-11}$	7.3×10^{-10}	6.8
Br_2	Br abstraction	$8 \pm 2 \times 10^{-12}$	6.7×10^{-10}	1.2
CH_3SSCH_3	thiomethylation	$1.2 \pm 0.2 \times 10^{-11}$	1.2×10^{-9}	0.96
$PhCH{=}CH_2$	addition	$1.20 \pm 0.03 \times 10^{-12}$	1.8×10^{-10}	0.65
$CHCl_3$	H abstraction	$4.1 \pm 0.6 \times 10^{-13}$	9.7×10^{-10}	0.042
$CHCl_3$	Cl abstraction	$6.5 \pm 1 \times 10^{-13}$	9.7×10^{-10}	0.067
$CDCl_3$	D abstraction	$3.5 \pm 0.9 \times 10^{-14}$	9.7×10^{-10}	0.0036
$CDCl_3$	Cl abstraction	$7.23 \pm 0.05 \times 10^{-13}$	9.7×10^{-10}	0.074
$CH_2{=}CH{-}CH_2Br$	Br abstraction	$5.3 \pm 0.4 \times 10^{-13}$	9.7×10^{-10}	0.055
$CH_2{=}CH{-}CH_2Br$	allylation	$2.5 \pm 0.1 \times 10^{-13}$	9.7×10^{-10}	0.026

a peroxyl radical. In the present study, the bridgehead radical **3** was observed to undergo a radical–radical combination with both (a) dioxygen and (b) nitric oxide (Scheme 5). Reaction of the radical **3** with ^{18}O-labelled dioxygen yields a major product of m/z 214, with a rate constant of 8.5×10^{-11} cm^3 molecule^{-1} s^{-1}. The product ion is ascribed the structure of doubly ^{18}O-labelled 3-carboxylato-1-adamantylperoxyl radical anion **13** and is formed with a reaction efficiency of 16%. Given that no kinetic barrier is expected in the formation of the peroxyl radical, the relatively low efficiency for this reaction reflects the ability of this alkyl peroxyl radical to accommodate the 169 kJ mol^{-1} of energy released by the formation of the nascent carbon–oxygen bond.[4] The kinetic isotope effect is expected to be small between the rate constants for reaction of **3** with $^{18}O_2$ and naturally abundant $^{16}O_2$. Consequently, the measured rate constant can be used in conjunction with the competing appearance of unlabelled peroxyl radicals at m/z 210 to estimate the background concentration of dioxygen within the ion trap to be $3.0 \pm 0.2 \times 10^9$ molecules cm^{-3}. This value is remarkably close to the crude estimate of 10^{10} molecules cm^{-3} presented in our previous communication.[4]

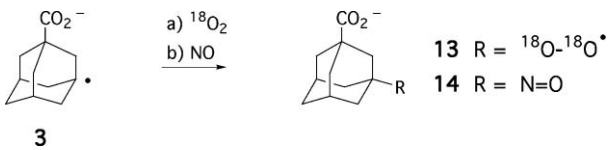

Scheme 5

Bayes and co-workers have previously measured the rate constants for the reaction of butyl radicals generated by laser flash photolysis with O_2 in the gas phase at room temperature by photoionisation mass spectrometry.[36] Their results for *n*-butyl (0.75 ± 0.14), *sec*-butyl (1.66 ± 0.22) and *tert*-butyl (2.34 ± 0.39 × 10^{-11} cm^3 molecule^{-1} s^{-1}) reveal the reactivity trend 3° > 2° > 1° and are of comparable magnitude to those obtained in the present study using the distonic radical anion approach. Furthermore, using simple hard sphere theory, we estimate the collision frequency for a *tert*-butyl radical with dioxygen at 298 K is 3.9×10^{-10} cm^3 molecule^{-1} s^{-1}, resulting in a reaction efficiency of 6.0%. This value is less than half that for the reaction of **3**, suggesting that the bridgehead radical is more reactive with oxygen than its planar cousin. Consistent with expectation from solution phase experiments, this comparison presents the first evidence for the enhanced reactivity of bridgehead radicals in the gas phase.

The reaction of **3** with nitric oxide produced an ion of m/z 208, assigned to be the 3-nitrosoadamantanecarboxylate anion **14**, with rate constant $3.84 \pm 0.04 \times 10^{-11}$ cm^3 molecule^{-1} s^{-1} and efficiency of about 6%. The addition of NO to the radical anion rather than the displacement of CO_2 (as previously observed by Wenthold and Squires for the acetate radical anion)[37] provides further support to the distonic character of **3**. No rate constant could be found in the literature for the reaction of a bridgehead radical with NO but previous studies of reactions of carbon-centred radicals with NO have been reported and represent an interesting comparison. The rate constant for the reaction of *tert*-butyl with NO determined by the muon spin relaxation technique is $1.0 \pm 0.3 \times 10^{-11}$ cm^3 molecule^{-1} s^{-1} and that for ethyl radical is $2.2 \pm 0.6 \times 10^{-11}$ cm^3 molecule^{-1} s^{-1} at 307 K.[38] A value of 3.5 ± 0.1 × 10^{-11} cm^3 molecule^{-1} s^{-1} was measured by colour centre laser kinetic spectroscopy for the reaction of ethynyl radical with NO[39] and $9.5 \pm 1.2 \times 10^{-12}$ cm^3 molecule^{-1} s^{-1} for benzyl radical with NO at 298 K by laser flash photolysis.[40] Our value compares favourably with these, with a rate constant *ca.* four times greater than that of *tert*-butyl, which could be accounted for by increased reactivity arising from bridgehead strain and from greater collision frequency arising from the ion–dipole interactions.

Substitution reactions

Radical **3** underwent substitution reactions with (a) iodine, (b) bromine, (c) dimethyl disulfide, (d) chloroform, (e) deuterochloroform and (f) allyl bromide (Scheme 6). The concentrations of bromine and iodine in the trap were estimated by measuring the mass decrease over time of the halogen in a sealed vial connected to the low pressure helium inlet to the trap. Uncertainties represent primarily those in the mass loss measurements. Formation of 3-iodo- **10** and 3-bromoadamantanecarboxylate anion **15** occurred

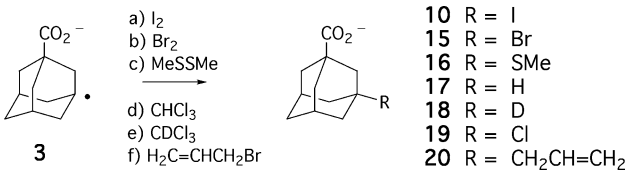

Scheme 6

with rate constants of $5 \pm 5 \times 10^{-11}$ and $8 \pm 2 \times 10^{-12}$ cm^3 molecule^{-1} s^{-1} respectively. Given that the rate constants could not be measured with high precision, it is difficult to establish with certainty which of the two is faster.

Kenttämaa and co-workers have previously used dimethyl disulfide (DMDS) as an effective probe of the distonic character of radical cations.[17] They have established that non-distonic (resonance stabilised) species are generally unreactive towards the reagent while distonic radical cations undergo a substitution reaction at sulfur resulting in formation of a thiomethyl ether. From the literature, however, the case for radical anions is less clear, but at face value one should expect comparable reactivity. Bridgehead radical **3** underwent a relatively rapid reaction ($k = 1.2 \pm 0.2 \times 10^{-11}$ cm^3 molecules^{-1} s^{-1}, $\Phi = 0.96\%$) with DMDS to yield an ion of m/z 225, assigned as the 3-methylthioadamantanecarboxylate anion **16**, demonstrating the ease with which methylthio radicals may be displaced in an S_H2 process. The observation of a CH_3S– adduct and the relative efficiency of this reaction is taken as additional evidence for the distonic structure of **3**. For comparison, distonic aryl radical anion 3-carboxylato-1-phenyl **7** reacts with DMDS with a rate constant of 8×10^{-12} cm^3 molecules^{-1} s^{-1} and efficiency of 0.5%.[15]

Chlorine atom abstraction from chloroform by **3** to form **19** is sluggish compared with most other reactions, but clearly consonant with Cl abstraction from $CDCl_3$ ($\Phi = 0.067$ and 0.074% respectively) as expected. A large primary kinetic isotope effect of $k_H/k_D = 13 \pm 2$ was evident for hydrogen/deuterium atom removal in the formation of **17** and **18** respectively. The ratio of abstraction of hydrogen to chlorine in chloroform was $k_H/k_{Cl} = 0.62$.

Both bromination and allylation of **3** with allyl bromide, forming **15** and **20** respectively, were relatively slow compared to other substitution processes, with alkylation being favoured by a factor of 2.1. Given the steric bulk of **3**, installation of the allyl group at the bridgehead carbon most likely occurs *via* an S_H2' mechanism,[41] with **3** attacking at the methylene of the double bond (Scheme 7a). Based on these data, however, a direct S_H2 reaction at the allylic position cannot be rigorously excluded (Scheme 7b).

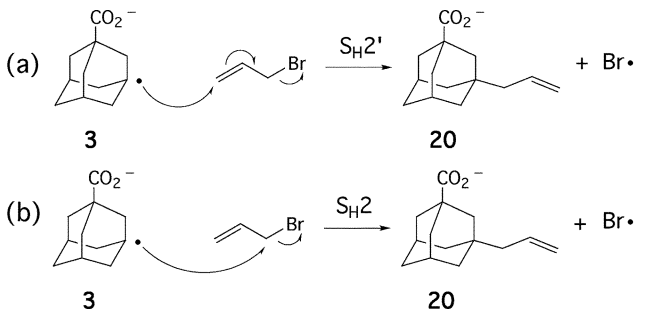

Scheme 7

Addition to carbon–carbon double bonds

Radical **3** underwent addition to styrene yielding a product ion of m/z 282, almost certainly the stabilised benzylic radical **21** (Scheme 8). This reaction appeared considerably slowed due to the decreased collision frequency resulting from the low polarity of styrene, but the efficiency was in fact two-thirds that for reaction of **3** with DMDS. A subsequent addition of styrene to **21**—an attempt

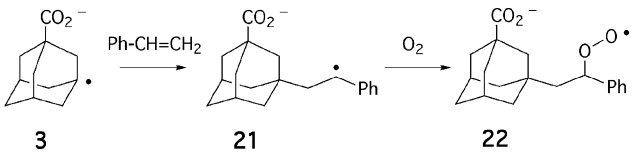

Scheme 8

at gas phase free radical polymerisation—was not observed, indicating that the resonance stabilised intermediate radical was considerably less reactive than the bridgehead radical initiator. However, addition of adventitious dioxygen to the benzylic radical to give peroxyl radical **22** was observed. Once formed, subsequent trapping of **21** gave amounts of m/z 314, the yields escalating with increasing reaction time. This process was considerably slower than the reaction of **3** with O_2, an estimate for k_2 being $2 \pm 1 \times 10^{-13}$ cm^3 molecule^{-1} s^{-1}.

Conclusion

Electrospray ionisation ion trap mass spectrometry has enabled generation of the distonic 3-carboxylato-1-adamantyl radical anion **3** from a readily prepared precursor and allowed the study of the radical reactions of this mass-selected bridgehead radical with neutral reagents. Strong evidence has been obtained for the intact bridgehead radical structure. Reaction with common reagents occurs in a manner expected from classic solution phase free radical chemistry, with radical–radical combination, addition to double bonds and substitution reactions observed. Rate data have been obtained for the first time for 12 reactions of **3** in the gas phase and represent the first gas phase rate data for any bridgehead radical. Rate constants spanned several orders of magnitude, the fastest reaction being the addition of $^{18}O_2$ (8.5×10^{-10} cm^3 molecule^{-1} s^{-1}) whose rate constant was 2400 times that for the abstraction of a deuterium atom from $CDCl_3$ (3.5×10^{-14}). A comparison of reaction efficiencies for the reactions of **3** and *tert*-butyl radical with dioxygen suggest that the pyramidal bridgehead species is more reactive than its near-planar relative.

Experimental

Reagents (AR grade) and solvents were obtained commercially, taken from freshly opened bottles and used without further purification, unless stated otherwise. $^{18}O_2$ gas (95%) was obtained from Cambridge Isotopes. DMF was dried over activated 3 Å molecular sieves. Crystalline *N*-hydroxypyridine-2-thione was obtained economically by treatment with concentrated HCl of a commercial 40% aqueous solution of sodium 2-mercaptopyridine *N*-oxide, as described previously.[42] Chloroform was run through silica gel to obtain a sample which was ethanol free. Allyl bromide was treated in the same manner to afford a colourless sample.

N-(1-Adamantanoyloxy-3-carboxylic acid)pyridine-2-thione

A general method[24] was adapted and performed under minimal light to minimise decomposition of the photolabile product. A stirred solution of 1,3-adamantanedicarboxylic acid (100 mg, 0.446 mmol) in 500 μL dry DMF was cooled to 0 °C. A solution of dicyclohexylcarbodiimide (94 mg, 0.46 mmol) and *N*-hydroxypyridine-2-thione (55 mg, 0.43 mmol) in 1.5 mL dry DMF

was added dropwise over 5 min. The mixture was allowed to warm to room temperature, stirred for an additional 8 h, then filtered to remove the insoluble dicyclohexyl urea. A further 2 mL DMF was used to rinse the precipitate. The filtrate was treated with 15 mL water, causing the yellow product to precipitate. After cooling to 0 °C, the product was collected by filtration, washed with 10 mL cold water and dried under vacuum to give a yellow solid (110 mg). A portion (40 mg) was purified by flash chromatography on silica, eluting with 20–40% (v/v) EtOAc in chloroform (R_f 0.34, 20% EtOAc), which yielded a yellow, crystalline solid (18 mg, 35%), mp 172.5–174 °C. Recrystallisation from $CHCl_3$–hexane gave yellow prisms of mp 176–177 °C. δ_H (500 MHz, CD_3SOCD_3) δ 1.76 (s, br, 2H), 2.08–2.11 (m, 8H), 2.26 (s, br, 2H), 2.44 (s, br, 2H), 6.88 (ddd, 1H), 7.43 (ddd, 1H), 7.54 (dd, 1H), 8.34 (dd, 1H), 12.20 (s, br, 1H). ν (neat powder)/cm^{-1} 3327, 2932, 2858, 1785, 1714 (s), 1699 (vs), 1626, 1610, 1576, 1529, 1454, 1413, 1276, 1232, 1132, 1053, 978, 906, 754.

3-Hydroxyadamantanecarboxylic acid 11

A published method[30] was altered slightly for convenience. KOH (4.955 g, 88.31 mmol) was dissolved in 200 mL water and 1-adamantanecarboxylic acid (20.0 g, 111 mmol) was dissolved portionwise in the stirred solution. $KMnO_4$ (20.0 g, 127 mmol) was added in several portions and the mixture was stirred overnight, then heated at 80 °C until it became brown in colour. After cooling to RT, concentrated H_2SO_4 was added (~30 mL), followed by 20 g (190 mmol) $NaHSO_3$ to destroy the MnO_2. An aqueous suspension of the white product resulted, which was treated with 20 g NaCl, then cooled to 0 °C, filtered and washed repeatedly with 10% aqueous H_2SO_4, then with cold water. After drying the product under vacuum (20.9 g, 96% crude), it was dissolved in 320 mL boiling EtOAc, hot filtered and allowed to recrystallise to yield white prisms (9.09 g, 42%) of mp 203–205.5 °C (lit.[30] 202–203 °C). A second crop (2.57 g, 12%) of mp 198–200 °C was obtained by concentration of the mother liquors. δ_H (300 MHz, CD_3SOCD_3) 1.47–1.52 (2H, m), 1.52–1.56 (4H, m), 1.62–1.67 (6H, m), 2.08–2.15 (2H, m), 4.49 (1H, s, br, OH), 12.01 (1H, s, br, COOH). δ_C (75 MHz, CD_3SOCD_3) 29.7 (2CH), 34.9, 37.6 (2C), 42.9 (quat), 44.3 (2C), 46.5, 66.3 (C–O), 177.7 (C=O). ν (neat powder)/cm^{-1} 3446, 2909, 1705 (vs), 1265 (vs), 1248 (vs), 1229, 1120, 1010, 941, 880, 723.

3-Bromoadamantanecarboxylic acid

3-Hydroxyadamantane-1-carboxylic acid (500 mg, 3.55 mmol) and 48% aqueous HBr (5.0 mL, 44 mmol) were placed in a capped reaction vial and stirred for 3.5 h at 90 °C. After cooling to 0 °C, the mixture was filtered and the precipitate washed with 5 mL cold water. The resulting product was dried under vacuum to yield white crystals (0.659 g, 99.8%), mp 144.5–146.5 °C (lit.[43] 145–146 °C), used without further purification. δ_H (500 MHz, $CDCl_3$) 1.65–1.74 (2H, m), 1.89–1.96 (4H, m), 2.21–2.23 (2H, m), 2.28–2.35 (4H, m), 2.48–2.53 (2H, m), 5.25 (1H, s, br, OH). δ_C (125 MHz, $CDCl_3$) 31.5 (2C), 34.4, 36.8 (2C), 44.6, 48.0 (2C), 49.3, 63.2 (C-Br), 181.7 (C=O). ν (neat powder)/cm^{-1} 3446, 2914, 2858, 1689 (vs), 1293, 1280, 1090, 948, 830, 768.

3-Iodoadamantanecarboxylic acid 12

3-Hydroxyadamantane-1-carboxylic acid (501 mg, 2.55 mmol) and 55% aqueous HI (5.0 mL, 66 mmol) were placed in a capped reaction vial and stirred for 16 h at 60 °C. After cooling to 0 °C, the mixture was filtered and the precipitate washed with 3 × 5 mL cold water to remove all colour from the product. After drying under vacuum, the yield of white crystals was 0.780 g (99.8%), mp 166–168 °C (lit.[44] 165 °C), and the sample was used without further purification. δ_H (500 MHz, $CDCl_3$) 1.75–1.82 (2H, m), 1.95–2.05 (4H, m), 2.02–2.12 (2H, m), 2.53–2.2.60 (4H, m), 2.71–2.79 (2H, m), 5.00 (1H, s, br, OH). δ_C (125 MHz, $CDCl_3$) 31.9 (2C), 34.4, 36.8 (2C), 44.6, 45.7 (C–I), 51.0 (2C), 52.2, 181.5 (C=O). ν (neat powder)/cm^{-1} 2934, 2904, 1704 (vs), 1450, 1413, 1332, 1283 (s), 1261 (s), 1233, 1076, 967, 893, 820.

Nitric oxide

Nitric oxide was generated and purified on a 50 mL scale by an ingeniously simple established method.[45] The reaction in a 60 mL capped disposable syringe between sodium nitrite (0.250 g, 3.62 mmol) and ferrous sulfate (3.0 mL of an aqueous solution 1.2 M in $FeSO_4$ and 1.6 M in H_2SO_4) produced about 60 mL of crude nitric oxide. After expulsion of the liquid, the gas was washed by drawing 5 mL of aqueous 1 M NaOH solution into the syringe and shaking. The base wash was expelled and the now colourless gas was washed further with 2 × 5 mL water, and then dried by passage into a second 60 mL syringe, through PVC tubing containing a plug of anhydrous $MgSO_4$.

Mass spectrometry

Mass spectra were obtained using a Finnigan (now ThermoFisher) LTQ quadrupole linear ion trap spectrometer (San Jose, CA).[28] Solutions of analytes at concentrations below 1 mM in HPLC grade methanol were subject to electrospray ionization (ESI) in negative mode. Capillary potentials were typically 3–4 kV. Once formed, anions were held in the ion trap at a manufacturer-stated pressure of ultrahigh purity helium (BOC, Australia) and reagent of 2.50 ± 0.20 mTorr. Pressure inside the trap was measured at 2.58 ± 0.13 mTorr using a known rate constant[25] for the reaction of bromide with methyl iodide (eqn (2)). Radical **3** was formed by mass selection of ion **5** (2–5 Th isolation window), followed by CID (25–35 arbitrary normalised collision energy units) for a time of 30 ms. Once formed, the ion isolation window for radical **3** was set to 2.0 Th to exclude isotope peaks and the *Q*-value set to 0.25 to ensure that the effective temperature inside the trap was not significantly elevated above ambient. Ions arriving from the ion optics were subjected to two trapping cycles prior to kinetic analysis to ensure their effective thermalisation with buffer gas. An acquisition of 100–200 scans was usually obtained and reaction times varied from 10 ms to 5 s.

Reagent molecules were provided to the linear trap atmosphere in known concentration in a manner similar to that reported by Gronert *et al.* for a 3-D trap instrument.[12] Mixtures of helium and reagent enter the trap inside the mass spectrometer *via* a nipple on the exit endcap electrode and exit *via* small holes in the entrance and exit endcap electrodes. A mixing system allowing the introduction of reagents into the helium stream was constructed (Fig. 2). A reagent (liquid or gas) is injected by pump-driven

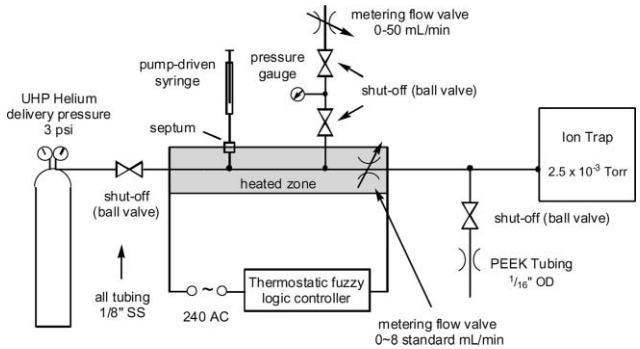

Fig. 2 A schematic drawing of the mixing system that permits the introduction of reagents into the ion trap mass spectrometer.

syringe into the helium gas (3–5 psi) flow. The stainless steel helium line (2 m) is wound around a copper bar fitted with a thermostatted 100 W electric heating element so as to allow heating (25–250 °C) of the gas flow if volatility of the reagent at room temperature is insufficient. A variable leak valve (Granville-Phillips Model 203, Boulder, Colorado) in the heated zone admits a flow of the reagent–helium mixture to the ion trap such that the pressure may be varied in the trap. A second metering valve can be used to vary the concentration of reagent by controlling the split flow, similar to a GC injector port. For admission of corrosive reagents or those possessing a very low vapour pressure, an inlet restricted with PEEK tubing is provided. The entire heated zone can be placed under vacuum to expedite removal of a reagent prior to the introduction of the next.

Kinetic measurements

At full capacity, the trap contains approximately 2×10^4 ions.[27,28] A practical concentration range for neutral reagents inside the trap is 10^9–10^{13} molecules cm^{-3} and the volume inside the trap is 13.5 cm^3.[27,28] Consequently, the molar ratio of neutral reagent to ions is of the order 10^6–10^{10}, clearly establishing the ions as the limiting species. Thus, bimolecular reactions of ions and neutral reagents display pseudo-first order kinetics.

True second order rate constants, k_2 (cm^3 molecule^{-1} s^{-1}) for the reactions of 1-adamantyl-3-carboxylate radical anion with each neutral reagent were obtained by Gronert's method[12] from the pseudo-first order rate constant, k_1 (s^{-1}) and the pressure of the neutral reagent in the ion trap, P_n (molecule cm^{-3}) according to eqn (5). Pseudo-first order rate constants, k_1 (s^{-1}) were obtained from a series of mass spectra, recorded as a function of reaction time between the radical ion (R) and neutral reagent. The reaction time is defined as the interval between the isolation of the selected ion and ejection of all ions from the trap for analysis. A plot of the natural logarithm of the abundance of the radical ion at m/z 178 as a proportion of the total signal abundance (initial abundance of R) against reaction time yielded a linear relationship, with slope of $-k_1$ (eqn (6)). Plots consisted usually of 8 data points and extended to 4–5 half lives. Pressure of the neutral reagent (P_n) for each reaction was calculated from the pressure inside the ion trap (P_T) and the respective molar flows and molecular weights of the helium damping gas and reagent, using eqn (7). The final term accounts for difference in effusion, since lighter molecules are removed more quickly from the trap into the surrounding vacuum chamber.

$$k_2 = \frac{k_1}{P_n} \tag{5}$$

$$\ln\left(\frac{[R^\bullet]_t}{[R^\bullet]_0}\right) = -k_1 + c \tag{6}$$

$$P_n = P_T \times \frac{\text{molar flow rate of neutral}}{\text{molar flow rate of helium}} \times \sqrt{\frac{\text{molar mass of neutral}}{\text{molar mass of helium}}} \tag{7}$$

It is known that for low Q values, the effective temperature of ions at equilibrium inside the trap is equivalent to ambient temperature.[31,32] The temperature of the case surrounding the ion trap was measured at 307 ± 1 K, which is taken as being the effective temperature for these experiments. In some instances, reaction of the radical with a neutral formed two or more products. If a secondary species was formed as a result of decomposition of a primary product, its concentration was attributed to that of the primary to ensure accurate kinetics. Formation of products by separate pathways was treated by a standard parallel pseudo-first order kinetics analysis. Collision rate coefficients for the ion–molecule reactions were estimated by average dipole orientation (ADO) theory[33] for 307 K. The dipole moment, molar mass and polarisability are required for the neutral and the charge and molar mass are required for the distonic ion. An available Fortran routine was used to facilitate these calculations.[34]

Acknowledgements

SJB and DGH acknowledge the Australian Research Council (DP0452849) and the University of Wollongong for funding. The authors acknowledge Mr Benjamin Kirk for computational assistance and Messrs Martin Riggenbach, Steven Cooper, Larry Hick and Peter Sarakiniotis for assistance in the design and construction of equipment. We gratefully acknowledge Professor Richard O'Hair, Drs George Khairallah and Tom Waters for helpful discussions regarding kinetic analyses and the design of instrument modifications.

References

1 J. C. Walton, *Chem. Soc. Rev.*, 1992, **21**, 105–112.
2 C. J. Rhodes, J. C. Walton and E. W. Della, *J. Chem. Soc., Perkin Trans. 2*, 1993, 2125–2128.
3 G. Yan, N. R. Brinkmann and H. F. Schaefer, *J. Phys. Chem. A*, 2003, **107**, 9479–9485.
4 D. G. Harman and S. J. Blanksby, *Chem. Commun.*, 2006, 859–861.
5 D. Griller, K. U. Ingold, P. J. Krusic and H. Fischer, *J. Am. Chem. Soc.*, 1978, **100**, 6750–6752.
6 J. Pacansky, W. Koch and M. D. Miller, *J. Am. Chem. Soc.*, 1991, **113**, 317–328.
7 B. Noller, R. Maksimenka, I. Fischer, M. Armone, B. Engels, C. Alcaraz, L. Poisson and J. M. Mestdagh, *J. Phys. Chem. A*, 2007, **111**, 1771–1779.
8 Y. Feng, L. Liu, J. T. Wang, S. W. Zhao and Q. X. Guo, *J. Org. Chem.*, 2004, **69**, 3129–3138.
9 I. Fleming, *Frontier Orbitals and Organic Chemical Reactions*, Wiley-Interscience, Chichester, 1976.
10 J. T. Banks, K. U. Ingold, E. W. Della and J. C. Walton, *Tetrahedron Lett.*, 1996, **37**, 8059–8060.

11 P. D. Lightfoot, R. A. Cox, J. N. Crowley, M. Destriau, G. D. Hayman, M. E. Jenkin, G. K. Moortgat and F. Zabel, *Atmos. Environ., Part A*, 1992, **26**, 1805–1961.
12 S. Gronert, L. M. Pratt and S. Mogali, *J. Am. Chem. Soc.*, 2001, **123**, 3081–3091.
13 T. Waters, R. A. J. O'Hair and A. G. Wedd, *J. Am. Chem. Soc.*, 2003, **125**, 3384–3396.
14 B. F. Yates, W. J. Bouma and L. Radom, *J. Am. Chem. Soc.*, 1984, **106**, 5805–5808.
15 C. J. Petzold, E. D. Nelson, H. A. Lardin and H. I. Kenttämaa, *J. Phys. Chem. A*, 2002, **106**, 9767–9775.
16 K. K. Thoen, R. L. Smith, J. J. Nousiainen, E. D. Nelson and H. I. Kenttämaa, *J. Am. Chem. Soc.*, 1996, **118**, 8669–8676.
17 K. M. Stirk, J. C. Orlowski, D. T. Leeck and H. I. Kenttämaa, *J. Am. Chem. Soc.*, 1992, **114**, 8604–8606.
18 D. R. Reed, M. Hare and S. R. Kass, *J. Am. Chem. Soc.*, 2000, **122**, 10689–10696.
19 A. Karnezis, C. K. Barlow, R. A. J. O'Hair and W. D. McFadyen, *Rapid Commun. Mass Spectrom.*, 2006, **20**, 2865–2870.
20 S. Wee, A. Mortimer, D. Moran, A. Wright, C. K. Barlow, R. A. J. O'Hair, L. Radom and C. J. Easton, *Chem. Commun.*, 2006, 4233–4235.
21 C. K. Barlow, S. Wee, W. D. McFadyen and R. A. J. O'Hair, *Dalton Trans.*, 2004, 3199–3204.
22 D. H. R. Barton, D. Crich and W. B. Motherwell, *J. Chem. Soc., Chem. Commun.*, 1983, 939–941.
23 E. W. Della and J. Tsanaktsidis, *Aust. J. Chem.*, 1989, **42**, 61–69.
24 D. H. R. Barton, J. MacKinnon, R. N. Perchet and C. L. Tse, Efficient synthesis of bromides from carboxylic acids containing a sensitive functional group: dec-9-enyl bromide from 10-undecenoic acid, in *Organic Syntheses, Collective Volumes*, ed. R. L. Danheiser, John Wiley & Sons, New York, 2004, vol. 10, p. 237.
25 S. Gronert, C. H. Depuy and V. M. Bierbaum, *J. Am. Chem. Soc.*, 1991, **113**, 4009–4010.
26 C. H. Depuy, S. Gronert, A. Mullin and V. M. Bierbaum, *J. Am. Chem. Soc.*, 1990, **112**, 8650–8655.
27 J. C. Schwartz, ThermoFisher, personal communication.
28 J. C. Schwartz, M. W. Senko and J. E. P. Syka, *J. Am. Soc. Mass Spectrom.*, 2002, **13**, 659–669.
29 F. F. Fenter, B. Noziere, F. Caralp and R. Lesclaux, *Int. J. Chem. Kinet.*, 1994, **26**, 171–189.
30 G. L. Anderson, W. A. Burks and Harruna, II, *Synth. Commun.*, 1988, **18**, 1967–1974.
31 A. V. Tolmachev, A. N. Vilkov, B. Bogdanov, L. Pasa-Tolic, C. D. Masselon and R. D. Smith, *J. Am. Soc. Mass Spectrom.*, 2004, **15**, 1616–1628.
32 S. Gronert, *J. Am. Soc. Mass Spectrom.*, 1998, **9**, 845–848.
33 T. Su and M. T. Bowers, Classical ion-molecule collision theory, in *Gas Phase Ion Chemistry*, ed. M. T. Bowers, Academic Press, New York, 1979, vol. 1, p. 83.
34 K. F. Lim, *Quantum Chemistry Program Exchange*, 1994, **14**, 3. The program Colrate (1994) is available for download from the author's website at Deakin University, Geelong, Victoria, Australia: http://www.deakin.edu.au/~lim/programs/COLRATE.html.
35 S. J. Yu, C. L. Holliman, D. L. Rempel and M. L. Gross, *J. Am. Chem. Soc.*, 1993, **115**, 9676–9682.
36 T. M. Lenhardt, C. E. McDade and K. D. Bayes, *J. Chem. Phys.*, 1980, **72**, 304–310.
37 P. G. Wenthold and R. R. Squires, *J. Am. Chem. Soc.*, 1994, **116**, 11890–11897.
38 H. Dilger, M. Stolmar, U. Himmer, E. Roduner and I. D. Reid, *J. Phys. Chem. A*, 1998, **102**, 6772–6777.
39 J. W. Stephens, J. L. Hall, H. Solka, W. B. Yan, R. F. Curl and G. P. Glass, *J. Phys. Chem.*, 1987, **91**, 5740–5743.
40 T. Ebata, K. Obi and I. Tanaka, *Chem. Phys. Lett.*, 1981, **77**, 480–483.
41 G. A. Russell, P. Ngoviwatchai and Y. W. Wu, *J. Am. Chem. Soc.*, 1989, **111**, 4921–4927.
42 D. H. R. Barton, D. Bridon, I. Fernandezpicot and S. Z. Zard, *Tetrahedron*, 1987, **43**, 2733–2740.
43 I. Handa and L. Bauer, *J. Chem. Eng. Data*, 1984, **29**, 223–225.
44 H. Stetter and J. Mayer, *Chem. Ber.*, 1962, **95**, 667–672.
45 (*a*) B. M. Mattson and J. Lannan, Microscale Gas Chemistry, Part 5. Experiments with Nitrogen Oxides, *Chem13 News*, 1997, Feb., 255; (*b*) B. M. Mattson, M. P. Anderson and S. E. Mattson, *Microscale Gas Chemistry*, 4th edn, Educational Innovations, 2006; (*c*) The author has instructions on his website (accessed last on 27 June 2007): http://mattson.creighton.edu/AllGases.html.